Deciphering the multiple effects of climate warming on the temporal shift of leaf unfolding

Haicheng Zhang, Isabelle Chuine, Pierre A.G. Regnier, Philippe Ciais, Wenping Yuan

Target journal: *Nature Climate Change*

Deciphering the multiple effects of climate warming on the temporal shift of leaf unfolding

Haicheng Zhang[1], Isabelle Chuine[2], Pierre Regnier[1], Philippe Ciais[3], Wenping Yuan[4]

[1]Department Geoscience, Environment & Society-BGEOSYS, Université libre de Bruxelles, B-1050 Bruxelles, Belgium.

[2] CEFE, CEFE, Université de Montpellier, CNRS, EPHE, IRD, Montpellier, FR-34293, cedex 5, France.

[3]Laboratoire des Sciences du Climat et de l'Environnement, IPSL-LSCECEA/CNRS/UVSQ Saclay, FR-91191 Gif-sur-Yvette, France.

[4]School of Atmospheric Sciences, Sun Yat-sen University, Zhuhai, Guangdong 510245, China.

Corresponding author: Haicheng Zhang (*haicheng.zhang@ulb.be*)

Abstract Changes in winter and spring temperatures have been widely used to explain the diverse responses of spring phenology to climate change. However, few studies have quantified their respective effects. Using 386,320 *in-situ* observations of leaf unfolding date (LUD) of six tree species in Europe, we show that the accelerated spring thermal accumulation and changes in winter chilling explain, on average, 61% and 39%, respectively, of the advancement of LUD during 1951–2019. We find that winter warming might not have delayed bud dormancy release, but instead it has increased the thermal requirement to reach leaf unfolding. The increase of thermal requirement and the decreased efficiency of spring warming to thermal accumulation partly explain the weakening response of leaf unfolding to warming. Our study stresses the need to better assess the antagonistic and heterogeneous effects of winter and spring warming on leaf phenology, which is key to projecting future vegetation-climate feedbacks.

Main

Timing of leaf unfolding influences the onset of the growing season of plants, and, therefore, vegetation productivity, as well as ecosystem water, carbon, and nutrient cycles[1-3]. Shifts in leaf unfolding date (LUD) may also alter competition between plant species and, thus, community structure at the decadal to centennial timescales, as well as the activities of insects and herbivores[4-6]. Many studies based on both *in situ* observations and satellite-derived data have reported a general trend of advancing spring leaf phenology during the past decades, in particular leaf unfolding, in response to climate warming in temperate and boreal regions[7-11]. However, although there is now mounting evidence that spring leaf phenology as a whole is shifting earlier in time, both the magnitude and direction of this shift show significant taxonomic, temporal and spatial variations[12-16]. In particular, the sensitivity of LUD to climate warming (S_T, day $°C^{-1}$), defined as the shift in LUD per °C, has significantly declined over the past 30 years in many regions[7,17].

Temperature has been regarded as the most important environmental factor controlling plant phenology in the extratropics[18]. Plants in these temperate and boreal regions generally require a certain number of cold days to break bud dormancy, and subsequently, a certain number of days with warmer conditions (called forcing temperatures) to trigger cell growth and leaf development[19-22]. Several studies have argued that changes in winter chilling and thermal accumulation caused by climate change explain the divergent shifts of LUD in response to rising temperature[7,23-26]. In particular, warming during winter can affect leaf unfolding through two distinct effects: it may delay the timing of bud dormancy release[27,28], and may increase the thermal requirement for bud break[20,29]. Both effects induce a delay in LUD. In contrast, spring warming accelerates thermal accumulation and cell growth, which has

55 an advancing effect on leaf unfolding. These opposing effects might explain why the
56 sensitivity of LUD to warming has significantly declined over the past 30 years[7,24];
57 they might also explain why some species have shown scant or no advances in LUD
58 with climate warming[8,23,25], as they may not be equally sensitive to both effects.

59 The impacts of climate warming on winter chilling and spring thermal accumulation
60 and, thus, on shifts in LUD, have not been quantitatively estimated for multiple
61 species at large spatial scales, particularly when considering the asynchronicity of
62 winter and spring warming[24,30,31]. Moreover, our mechanistic understanding of the
63 shifts in LUD in response to warming is still far from complete[32], especially regarding
64 the reported decline in the sensitivity of LUD to continuously rising temperature[7,33].
65 This limits our ability to project regional and global changes in LUD under future
66 climate warming, as well as the resulting changes in ecosystem structure and
67 functions.

68 Here, we take a new step to advance our quantitative and mechanistic understanding
69 of ongoing changes in leaf phenology. Using long-term (1951-2019) *in-situ*
70 observation data of LUD for six dominant broadleaved tree species (*Aesculus*
71 *hippocastanum*, *Alnus glutinosa*, *Betula pendula*, *Fagus sylvatica*, *Fraxinus excelsior*
72 and *Quercus robur*, Table S1) collected at 2944 sites in central Europe[34] (see Methods
73 and Extended Data Fig. 1), this study aims to: 1) quantify the relative contribution of
74 winter and spring warming to the temporal shifts in LUD in Europe; and 2) explore
75 the mechanisms that can explain the declining sensitivity of LUD to rising
76 temperature, as reported over the past decade[7].

77 To achieve these aims, we applied a process-based phenology model[19,28] at each of the
78 2944 observation sites for each tree species (see Methods). This type of models

describe known causal relationships between winter and spring temperatures and bud development[35,36]. Classical phenology models (e.g. Thermal Time, Sequential, Parallel and Alternating) generally rely on distinct assumptions (see Methods) regarding the response of bud growth to spring thermal accumulation and/or winter chilling[35,36]. As these models are non-nested, they cannot be used to test the effects of different assumptions on the response of leaf unfolding to chilling and forcing temperatures simultaneously[19]. To circumvent this limitation, we selected the Unified model as it integrates the different assumptions, and can be simplified by relaxing some of the hypotheses based on the parameter estimates obtained when the model is fitted to observed LUDs using inverse modelling and optimisation algorithms (see Methods and Supplementary Fig. S1). A previous study found more accurate predictions of LUD in Europe with the Unified model than other commonly used models[7]. We therefore used this model to disentangle the various effects of climate warming on leaf unfolding.

Contributions of winter and spring warming to LUD shifts

Based on *in-situ* observations, the average LUD in Europe advanced by 1.9 (±2.3, standard deviation of the shifts in LUD for all species across all observation sites, SD) and 5.8 (±2.9) days for the periods 1980–1999 and 2000–2019, respectively, compared to the reference period 1951–1979 (ΔLUD, Fig. 1a & Extended Data Fig. 2). Changes in LUD over time were similar across the six broadleaf species analysed, with differences between species in mean advancement of LUD at each site rarely exceeding one day for both periods. Yet, for all six species, there were larger differences in LUD shifts across sites, ranging from an advance of more than 10 days to a delay of more than 2 days (Extended Data Figs. 2 & 3). Generally, advances in LUD occurred more often at sites with stronger warming (e.g. northern Germany),

while delays in LUD mostly occurred at sites with temperature declines (e.g. south-eastern Germany and Austria) in the period 1951–2019 (Extended Data Figs. 3, 4 & Fig. S2). The average advance of LUD to 1°C rise (S_T) in mean annual, mean spring and mean winter temperatures in central Europe was 4.4 (±1.8), 3.2 (±1.2) and 1.4 (±0.7) days, respectively (Extended Data Fig. 5).

Overall, the Unified model (see Methods and Table S2) captured the observed LUDs of the six tree species included in this study (Extended Data Fig. 6, Figs. S3 & S4). The average root mean square error (RMSE) of all simulated LUDs was 5.8 days (Fig. S3), which is shorter than the observation interval (7 days) of the phenological data used in this study[33], highlighting that uncertainties in simulated LUDs might partly be due to uncertainties in observed LUDs. The model explained 65–78% of the spatiotemporal variations in LUD, depending on the species (Extended Data Fig. 6). The RMSE of predicted LUD for each of the six species showed no significant trend across time series and latitude (Fig. S4). The estimated optimal chilling temperature (T_{op}, °C) mostly varied between 3 and 10°C, with a mean value of 6.5 (±2.1)°C (Extended Data Fig. 7c), which is similar to values obtained with experimental data (2.5–9.1°C)[37-39].

According to the Unified model[19] (see Methods for details), bud dormancy is assumed to be released when chilling accumulation meets plants' critical requirements (CHA_0 in Fig. S1). The forcing stage starts as soon as this chilling requirement is met, and leaf unfolding occurs when the thermal accumulation during the forcing stage exceeds a given threshold. This threshold, denoted by TA_0, declines exponentially with the total amount of chilling received during the whole pre-growing season (CHA_{tot}, Fig. S1b), defined as the period from the onset of chilling accumulation to leaf unfolding. Therefore, the temporal shifts in LUD are determined by the time when bud dormancy

is released (d_{f0}), which in turn depends on the chilling accumulation rate (CH_r, Eq. 1), the thermal accumulation rate (F_r, Eq. 2), and the required amount of thermal accumulation (TA_0, Eq. 3), the latter being contingent on CHA_{tot} (Eq. 4) before leaf unfolding (Fig. S1).

Our results show that advances in LUD were mainly caused by the acceleration in thermal accumulation induced by the spring warming (ΔD_{Fr}, Figs. 1a & Extended Data Fig. 8). For the periods 1980–1999 and 2000–2019, the forcing stage duration was, respectively, 4.0 (±3.8) and 8.7 (±7.0) days shorter than in the reference period (1951–1979). In contrast, the increase TA_0 induced by the decline in CHA_{tot} delayed LUD by 1.2 (±1.6) and 2.3 (±2.0) days in 1981–2000 and 2000–2019, respectively, compared to the earlier period (ΔD_{TA0}, Fig. 1a). Changes in dormancy release day (ΔD_{df0}), which is also the onset of the forcing stage, contributed less to the shifts in LUD, generally by less than 2 days. From the period 1951–1979 to 1980–1999 and 2000–2019, the dormancy release day advanced, on average, by 0.3 (±2.1) and 1.7 (±3.9) days, respectively (Fig. 1a). Temporal shifts in dormancy release day differed significantly across species and were overall greater for *Fraxinus excelsior* (*Fe*) and *Quercus robur* (*Qr*), which have comparatively later LUDs (Fig. S5) than other species (Fig. 1 & Extended Data Fig. 2). Overall, ΔD_{Fr}, ΔD_{TA0} and ΔD_{df0} explained 61%, 22%, and 17% (Eqs. 12–14) of the total advance in LUD between the reference period (1951–1979) and the most recent period (2000–2019) (Fig. 1b). In other words, the acceleration in thermal accumulation caused by climate warming (ΔD_{Fr}) explained 61% of the temporal shift in LUD, while changes in chilling accumulation ($\Delta D_{df0}+\Delta D_{TA0}$) explained the remaining 39% through their influence on plants' thermal requirement and dormancy release date (Fig. 1b).

Revealing the antagonistic effects of temperature on LUD

154 The warming-induced change in the dormancy release day has been widely invoked to
155 explain why the LUDs of some plants show a weak or even delayed shift with climate
156 warming[7,8,16]. A common hypothesis relies on the premise that warm temperatures in
157 winter delay the timing at which the chilling requirement for dormancy release is met,
158 thus postponing the start of the forcing stage and mitigating the advancement of the
159 LUD. However, our results suggest that the winter warming only marginally changed
160 the timing of dormancy release, especially from 1951–1979 to 1980–1999 (Fig. 1). At
161 most of the observation sites, the optimized response functions to chilling temperature
162 showed an optimum (see the pattern plotted in Fig. S6b), in contrast to the widely
163 used index-chilling days[20,36] (Fig. S6a), which assumes a uniform effect of chilling
164 temperatures as long as they remain below a certain threshold. Winter temperatures
165 recorded at the observation sites were mostly 3–12°C lower than the local optimal
166 chilling temperature (T_{op}, °C) in the period 1951–1979, and then gradually increased
167 towards T_{op} with time (Fig. 2a). This decreasing difference between winter
168 temperature and optimal chilling temperatures translated into an important increase in
169 the chilling rates during winter (e.g. between days d_{c1} and d_{c2} in Fig. 3). On the
170 contrary, in late autumn and early spring, chilling tended to decrease because the
171 temperature tended to be higher than T_{op} (e.g. before d_{c1} and after d_{c2} in Fig. 3).
172 However, the increased chilling rate during winter partly or sometimes even fully,
173 offset the decreased chilling rates in late autumn. This explains why the dormancy
174 release days (ΔD_{df0}) were not substantially postponed and mostly occurred slightly
175 earlier for the six species investigated (Fig. 1).

176 The decrease in chilling accumulation rate in early spring between 1951–1979 and
177 2000–2019 (due to spring warming which caused the temperature to increase above
178 T_{op}, Figs. 2b & 3) resulted in an overall decrease in the total amount of chilling

accumulated before bud break (Fig. 2c). As a result, while dormancy could be released earlier, due to more efficient winter chilling during the most recent decades, total chilling accumulation nonetheless declined by 0.8 (±0.9)%, on average, from 1951–1979 to 1980–1999, and by 2.0 (±1.2)% from 1951–1979 to 2000–2019 (Fig. 2c). This decline translates into a slight but significant increase in the critical forcing accumulation required for leaf unfolding (TA0), by 0.5(±0.5) and 1.2(±0.8)% between the reference period and 1981–2010 and 2000–2019, respectively (Fig. 2d). However, this slight increase in TA0 was largely compensated by an increase in the forcing rate (F_{rave}, Fig. 2e) during spring of 8.9(±10.4) and 22.9(±13.9)% between the reference period and 1981–2010 and 2000–2019 periods, respectively. Thus, despite being higher, the plants' thermal requirements were reached within a shorter time interval in recent decades compared to the reference period, resulting in a significant advancement of the LUD (Fig. 1).

Explaining the declining sensitivity of LUD to warming

Consistent with previous studies conducted in Europe and China[7,17], we found a general decline in temperature sensitivity of LUD (S_T), although this decline seems to have stopped in the last 20 years in central Europe (Extended Data Fig. 9). The average daily chilling rate during the dormancy stage (Fig. 3, CH_{rave} from d_{c0} to d_{f0}) and the total chilling accumulation during the whole pre-growing season (Fig. 3, CHA_{tot} from d_{c0} to LUD), which together represent the overall impacts of winter chilling on leaf unfolding, explained 33.4(±21.5)% (mean±standard deviation) of the temporal variation in S_T. The average daily forcing rate (F_{rave} from d_{f0} to LUD) explained 21.0(±20.5)% of the temporal variation of S_T, on average (Fig. 4). The three metrics CH_{rave}, CHA_{tot}, and F_{rave} together accounted for 44.5(±21.0)% of the variation in S_T. Irrespective of the metrics, their explanatory powers varied drastically among

observation sites, as demonstrated by the large interquartile and 95% confidence intervals of R^2 in Fig. 4. This finding suggests that the metrics of controlling S_T might differ across observation sites. Note that the pre-growing season used to calculate S_T here (Fig. 4) is defined as the period from d_{c0} to LUD and thus differs from that applied in several previous studies[7,17,40], in which the pre-growing season was usually defined as the period for which the absolute value of the correlation coefficient between LUD and air temperature was largest (i.e. the period which is most relevant to leaf unfolding, see Methods). Nevertheless, calculating the pre-growing season this way provided similar results (Figs. 4 & S7).

Changes in winter chilling due to warming have been proposed as the main explanation for the temporal variation in S_T[7,17]. Our results show that the overall effect of winter warming on S_T is indeed higher than that of spring warming. Our results further support the hypothesis that winter warming leads to a decline in S_T by reducing the total amount of chilling received by the plants and subsequently increasing the critical forcing requirements for leaf unfolding (Figs. 2, 4 & Eq. 3). However, our findings do not support the hypothesis that winter warming leads to a decline in S_T by delaying the timing of dormancy release (d_{f0}). Indeed, although changes in CH_{rave} due to winter warming can induce changes in d_{f0} (Fig. 2), which would explain a decrease in S_T (Fig. 4), we found very limited changes in CH_{rave} and d_{f0}. In fact, at many observation sites, d_{f0} occurred slightly earlier, and not later, in response to the winter warming (Fig. 1).

We also draw attention to another cause of decreasing S_T with progressive warming. The response function to temperature during bud growth (forcing) was not linear at most sites (Fig. S1a), contrary to the widely used degree-day (defined as the difference between daily mean temperature and a base temperature, e.g. Fig. S14d).

Therefore, the effects of warming on accelerating forcing accumulation increases as temperature moves towards T_{50} (the temperature inducing 50% of optimal growth, the inflection point of the function), but decreases as temperature moves away from T_{50}. Estimates of T_{50} in Europe mostly varied between 8 and 11°C, on average (Fig. S7). While the temperature during the forcing stage was, on average, 0.35(±2.36) °C lower than T_{50} for the period 1951–1979 (Fig. 5), it was 0.08(±2.28) and 1.55(±2.51) °C higher for the periods 1980–1999 and 2000–2019 respectively. Therefore, spring mean temperature moved towards T_{50} from 1951–1979 to 1980–1999, while it moved away from it afterwards; this explains why the effect of warming on accelerating forcing accumulation decreased in the last 20 years while it had increased in the earlier periods (Fig. 1).

Although temperature is the dominant factor of spring phenology[18], the various temperature effects on LUD explain less than half of the temporal changes in S_T at many sites (Fig. 4). Other factors may also influence the response of leaf unfolding to climate warming in some species[5,41,42]. Temperature can vary strongly within a short time (e.g. a few days) and may show large interannual variations contrary to the photoperiodic cue. The latter is often viewed as an insurance against untimely bud break that could lead to fatal consequences (e.g. frost damage) during autumn and winter[43]. Nonetheless, we found that incorporating photoperiod (see Methods) into the Unified model significantly improved the performance of the model in capturing LUD at only a few locations (Extended Data Fig. 10), even for *Fagus sylvatica*, which has been reported as one of the most sensitive species to photoperiod[44,45], although there was a very modest decrease of the model error (Extended Data Fig. 10). Besides photoperiod, some studies suggest that frosts in late winter and early spring might exert a strong control on the bud phenology of several specific species[46-48]. In semi-

arid and arid regions, bud phenology may also be strongly affected by precipitation[49, 50]. Changes in such environmental factors might explain why the predictive power of temperature to explain temporal changes in S_T is not greater (Fig. 4). In addition, we found that the relationships between temperature sensitivity of leaf unfolding and the duration of the forcing stage and the forcing rate might be nonlinear at many sites (e.g. Fig. S8). Using linear regression functions may therefore underestimate the impacts of these variables on the temporal variation of S_T.

We also recognize that there might be some uncertainties in our results. First, our findings are based on phenological observations from central Europe, and they may not hold true for other regions. Second, temperature data were obtained from gridded databases (see Methods). Although the spatial resolution is high (0.1°) and the temperature was adjusted to the elevation of the sites with a temperature lapse rate, the temperature data still might be different from the actual temperature at the forest canopy. For example, some meteorological phenomena, such as air temperature inversion or the effect of topography on local air circulation and land–atmosphere feedbacks, can hardly be accounted for by a simple lapse rate[51,52]. Third, although the Unified model integrates most of the up-to-date known causal relationships between temperature and bud development[19], it may still miss some unknown mechanisms affecting bud phenology. Finally, the Unified model was calibrated using observed LUDs but without information on bud dormancy break date because no observation data of the imperceptible bud development processes for multiple trees at large scale are available yet. More experimental observation on the imperceptible phenological phases will be very helpful to further calibrate model parameters and evaluate the simulation results.

In this study, we showed that the overall effect of winter warming explained most of the decline in the sensitivity of leaf unfolding to temperature in Europe from 1951 to 2019, although not through a delayed dormancy break date. Additionally, we showed that spring warming explained part of the decline in the temperature sensitivity of LUD because of a smaller increase in forcing rate per degree of warming in recent decades. Our results reveal the importance of representing the antagonistic effects of chilling and forcing temperatures on bud development, as well as their heterogeneous effectiveness, especially when considering the seasonally uneven climate change[30,31]. We conclude that temperature sensitivity of leaf unfolding, calculated with a linear regression of LUD over mean pre-season temperature, is not a reliable index to project the response of plant phenology to future climate change. We call for further studies based on field observations and controlled condition experiments to deepen our understanding of the mechanisms driving plant phenology in a larger range of climatic conditions.

Acknowledgements

HZ and PR acknowledge the 'Lateral-CNP' project (No. 34823748) supported by the Fonds de la Recherche Scientifique –FNRS and the European Union's Horizon 2020 research and innovation program under grant agreements no. 776810 (VERIFY) and no. 101003536 (ESM2025– Earth System Models for the Future). WY is funded by the CAS interdisciplinary team (JCTD-2020-05). We acknowledge all members of the PEP725 network for collecting and providing the phenological data.

Author contributions

H.Z. and I.C. designed this study. H.Z. performed the specific simulation and data analysis. H.Z., P.R. and I.C. wrote most of the manuscript, with substantial contributions from P.C. and W.Y. All authors reviewed and revised the manuscript.

Competing interests

The authors declare no competing interests.

Figure Legends

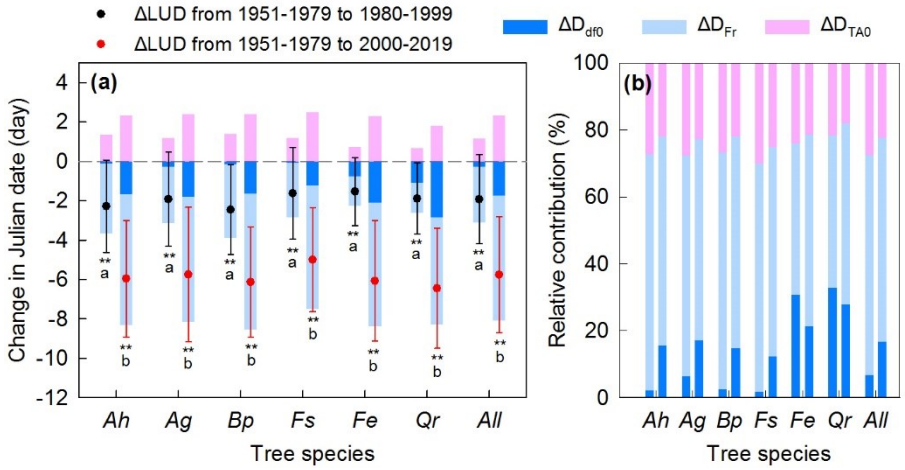

Figure 1 | Contribution of changes in winter chilling and spring forcing to changes in the LUDs of six tree species in Europe from 1951 to 2019. (a) and (b) show the absolute (Eqs. 6–11 in Methods) and relative (Eqs. 12–14 in Methods) contributions, respectively, of winter chilling and spring forcing to the changes in leaf unfolding date (ΔLUD). The negative and positive values denote an advance and a delay in LUD, respectively. ΔD_{df0} is the change in date when dormancy is released. ΔD_{Fr} is the potential change in the duration of the forcing stage caused by change in spring forcing temperatures. ΔD_{TA0} is the potential shift in LUD caused by change in plants' critical requirement for thermal accumulation. The black dot shows the average change in LUD from 1951–1979 to 1980–1999, and the red dot shows the average change in LUD from 1951–1979 to 2000–2019. Error bar denotes the standard deviation of ΔLUD across observation sites. ** indicates that the changes in LUD are significantly different from zero (p<0.05 based on one-sample t-test); and for each species, the different letters (a, b) below asterisks means that the changes in LUDs from 1951–1979 to 1980–1999 are significantly different from the changes from 1951–1979 to 2000–2019 (p<0.05 based on the paired-samples t-test). *AH*: *Aesculus hippocastanum*; *AG*: *Alnus glutinosa*; *BP*: *Betula pendula*; *FS*: *Fagus sylvatica*; *FE*: *Fraxinus excelsior*; *QR*: *Quercus robur*; *All*: the average value for all the six species.

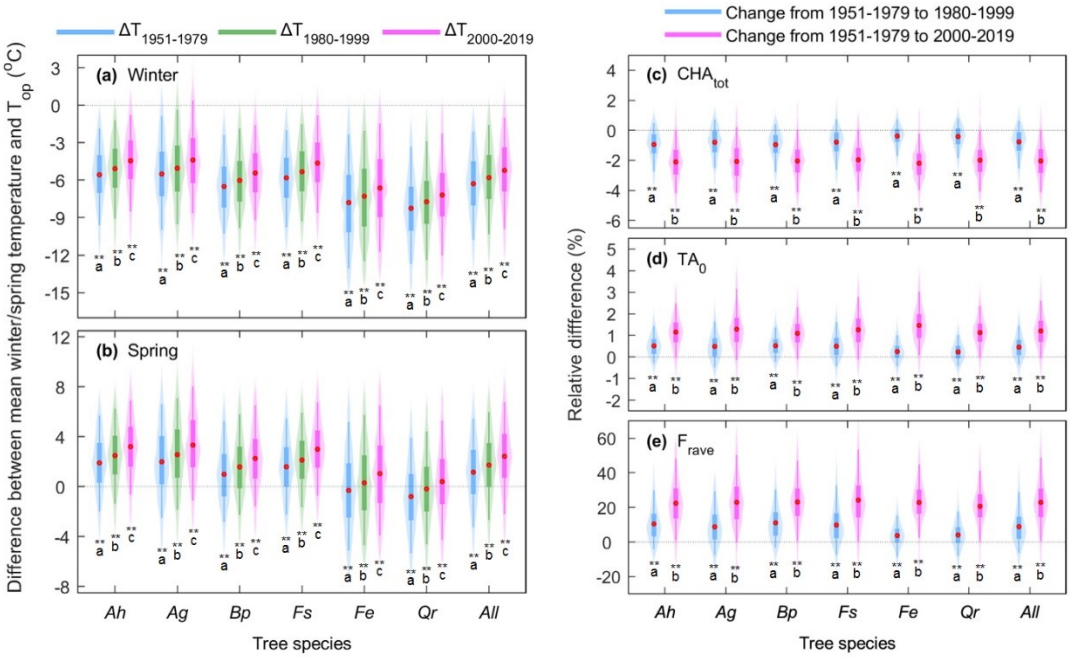

331

332 **Figure 2 | Differences between mean winter (December-February), mean spring**
333 **(March-May) temperatures and the optimal chilling temperature T_{op} (°C), and**
334 **the relative changes in different chilling and forcing metrics from 1951–1979 to**
335 **1980–1999 and 2000–2019.** CHA_{tot} is the total chilling accumulation (c); TA_0 is the
336 critical forcing accumulation required for leaf unfolding (d); and F_{rave} is the average
337 daily forcing rate during forcing stage (e). In each violin plot, the red dot refers to the
338 mean value and the balloon represents the probability density distribution of each
339 value. Whiskers indicate the interquartile (thick vertical bars) and 95 % confidence
340 intervals (thin vertical bars). The asterisks (**) indicate that the differences between
341 winter/spring temperatures and T_{op} (a,b) and the relative changes in CHA_{tot} (c), TA_0
342 (d) and F_{rave} (e) are significantly different from 0 ($p < 0.05$ based on one-sample t-
343 test). For each plant species, the violins marked with different letters (i.e. a, b and c
344 below the asterisks) are significantly different ($p<0.05$ based on the paired-samples t-
345 test). *AH*: *Aesculus hippocastanum*; *AG*: *Alnus glutinosa*; *BP*: *Betula pendula*; *FS*:
346 *Fagus sylvatica*; *FE*: *Fraxinus excelsior*; *QR*: *Quercus robur*; *All*: the average value
347 for all of the six species.

348

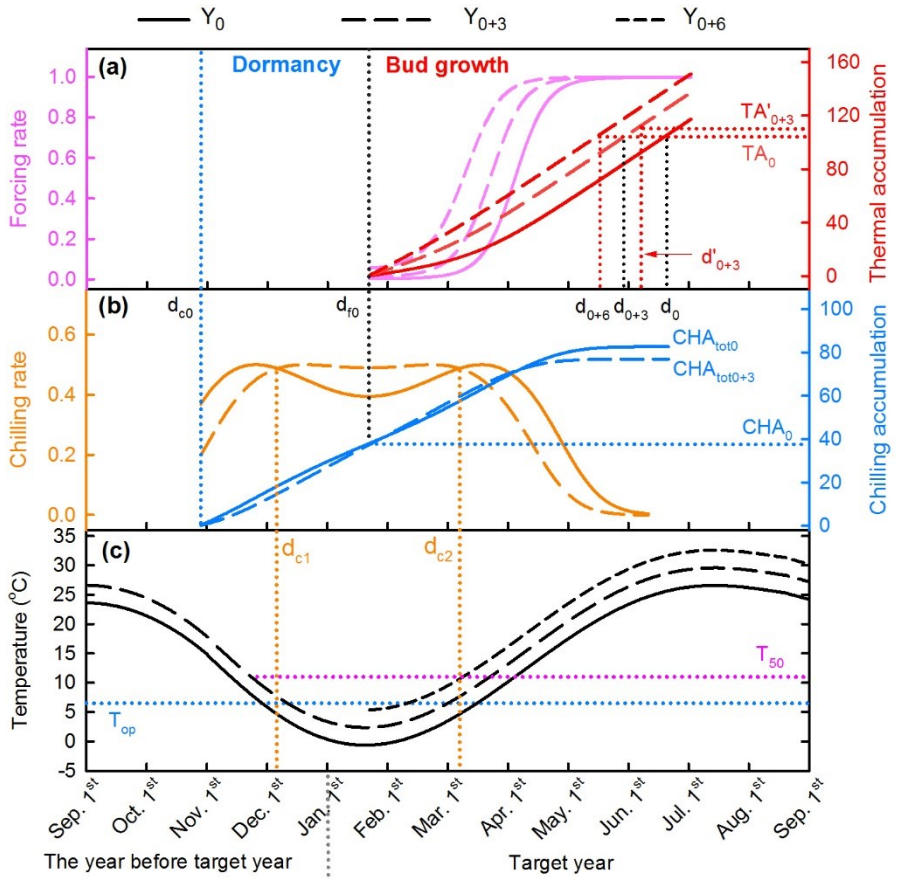

Figure 3 | Schematic plot showing the impacts of rising temperatures (+3 and +6 °C) on winter chilling, spring forcing and leaf unfolding date. T_{op} is the optimal chilling temperature (°C, Eq. 1); T_{50} is the mid-response temperature of daily forcing rate (°C, Eq. 2); CHA_0 is the critical chilling requirement for releasing dormancy; CHA_{tot0} and CHA_{tot+3} are the total chilling accumulation during the reference year (Y_0) and during an hypothetical year with 3 °C warming (Y_{0+3}); TA_0 and TA_{+3} are the corresponding critical forcing requirements for leaf unfolding. d_{c0} and d_{f0} are the respective start dates of chilling and forcing accumulation in the reference year (Y_0). d_0, d_{0+3} and d_{0+6} are the LUDs in the reference year Y_0 and in the years with +3°C and +6°C warming if the chilling accumulation would have been identical to the reference year (CHA_{tot0}). d'_{0+3} is the LUD in Y_{0+3} when considering the lower chilling accumulation (CHA_{tot+3}) induced by warming, and which leads to a higher forcing requirements. d_{c1} and d_{c2} represent the start and end dates of the period when temperatures in Y_{0+3} are more efficient for the chilling rate (because they are closer to T_{op}) than the temperatures in Y_0.

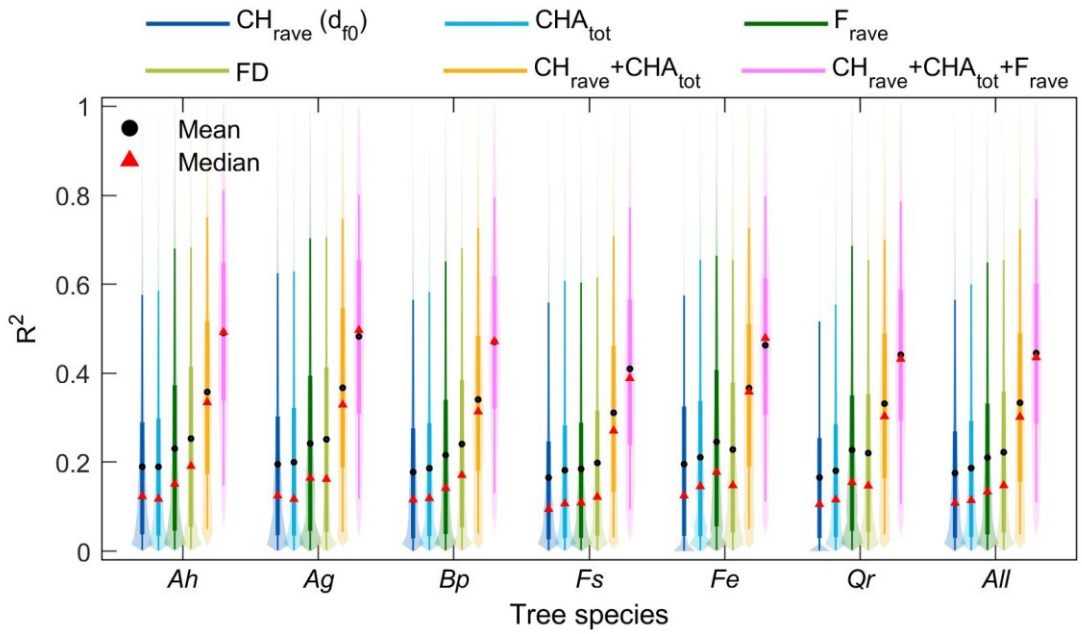

366

367 **Figure 4 | Coefficients of determination (R^2) for the linear regression function**
368 **between the temperature sensitivity of LUD and different metrics of winter**
369 **chilling and spring forcing.** The metrics are: CH_{rave}, the average daily chilling rate
370 from the start date of chilling accumulation (d_{c0} in Fig. 3) to the start date of forcing
371 accumulation (d_{f0} in Fig. 3); CHA_{tot}, the total chilling accumulation in the whole pre-
372 growing season; F_{rave}, the average daily forcing rate during the forcing stage; and DF,
373 the duration of forcing stage (day). In addition, CH_{rave} +CHA_{tot} refers to the regression
374 using both CH_{rave} and CHA_{tot} as independent variables, and CH_{rave} +CHA_{tot} +F_{rave}
375 refers to the regression using CH_{rave}, CHA_{tot} and F_{rave} together as independent
376 variables. In each violin plot, the balloon represents the probability density
377 distribution of each gradient of R^2. Whiskers indicate the interquartile (thick vertical
378 bars) and 95 % confidence intervals (thin vertical bars). *AH*: *Aesculus hippocastanum*;
379 *AG*: *Alnus glutinosa*; *BP*: *Betula pendula*; *FS*: *Fagus sylvatica*; *FE*: *Fraxinus*
380 *excelsior*; *QR*: *Quercus robur*; *All*: the average value for all of the six species.

381

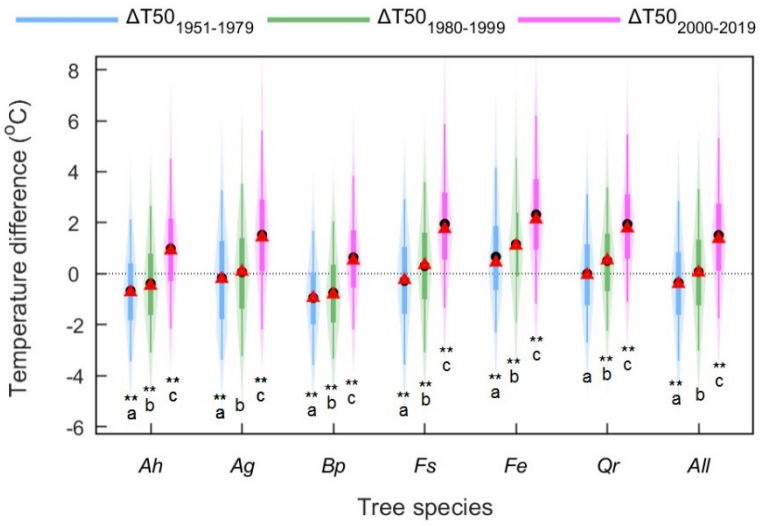

382

383 **Figure 5 | Differences between mean temperature during the forcing stage and**
384 **the mid-response temperature T_{50} (°C).** $\Delta T50_{1951\text{-}1979}$, $\Delta T50_{1980\text{-}1999}$ and $\Delta T50_{2000\text{-}2019}$ denote the difference between mean forcing stage temperature and T_{50} during the
386 periods 1951–1979, 1980–1999 and 2000–2019, respectively. Black and Red dots
387 denotes the mean and median value, respectively. The balloon represents the
388 probability density distribution of each value. Whiskers indicate the interquartile
389 (thick vertical bars) and 95 % confidence intervals (thin vertical bars). The asterisks
390 (**) indicate that the mean temperatures during forcing stage are significantly
391 different from the mid-response temperature T_{50} (p<0.05 based on one-sample t-test).
392 For each species, the different letters (a, b, c) below asterisks means the mean
393 temperatures during forcing stage are significantly different during the periods 1951–
394 1979, 1980–1999 and 2000–2019 (p<0.05 based on the paired-samples t-test). *AH*:
395 *Aesculus hippocastanum*; *AG*: *Alnus glutinosa*; *BP*: *Betula pendula*; *FS*: *Fagus*
396 *sylvatica*; *FE*: *Fraxinus excelsior*; *QR*: *Quercus robur*; *All*: the average value for all of
397 the six species.

398

References

1. Arora, V. K. & Boer, G. J. A. parameterization of leaf phenology for the terrestrial ecosystem component of climate models. *Glob. Change Biol.***11**, 39-59 (2005).
2. Richardson, A. D. *et al.* Terrestrial biosphere models need better representation of vegetation phenology: results from the North American Carbon Program Site Synthesis. *Glob. Change Biol.* **18**, 566-584 (2012).
3. Peñuelas, J., Rutishauser, T. & Filella, I. Phenology feedbacks on climate change. *Science* **324**, 887-888 (2009).
4. Richardson, A. D. *et al.* Influence of spring and autumn phenological transitions on forest ecosystem productivity. *Philos. Trans. R. Soc. B Biol. Sci.* **365**, 3227-3246 (2010).
5. Diez, J. M. *et al.* Forecasting phenology: from species variability to community patterns. *Ecol Lett* **15**, 545-553 (2012).
6. Hegland, S. J., Nielsen, A., Lazaro, A., Bjerknes, A. L. & Totland, O. How does climate warming affect plant-pollinator interactions? *Ecol. Lett.* **12**, 184-195 (2009).
7. Fu, Y. H. *et al.* Declining global warming effects on the phenology of spring leaf unfolding. *Nature* **526**, 104-107 (2015).
8. Zhang, H., Yuan, W., Liu, S. & Dong, W. Divergent responses of leaf phenology to changing temperature among plant species and geographical regions. *Ecosphere* **6**, art250 (2015); doi:10.1890/es15-00223.1
9. Zhang, G., Zhang, Y., Dong, J. & Xiao, X. Green-up dates in the Tibetan Plateau have continuously advanced from 1982 to 2011. *Proc. Natl. Acad. Sci. USA* **110**, 4309-4314 (2013).
10. Menzel, A. *et al.* European phenological response to climate change matches the warming pattern. *Glob. Change Biol.* **12**, 1969-1976 (2006).
11. Cleland, E. E., Chuine, I., Menzel, A., Mooney, H. A. & Schwartz, M. D. Shifting plant phenology in response to global change. *Trends Ecol. Evol.* **22**, 357-365 (2007).
12. Menzel, A., Sparks, T. H., Estrella, N. & Roy, D. B. Altered geographic and temporal variability in phenology in response to climate change. *Glob. Ecol. Biogeogr.* **15**, 498-504 (2006).
13. Zhang, X., Tarpley, D. & Sullivan, J. T. Diverse responses of vegetation phenology to a warming climate. *Geophys. Res. Lett.* **34**, (2007); doi:10.1029/2007gl031447
14. Fitter, A. H. & Fitter, R. S. Rapid changes in flowering time in British plants. *Science* **296**, 1689-1691 (2002).
15. Primack, R. B. *et al.* Spatial and interspecific variability in phenological responses to warming temperatures. *Biol. Conserv.* **142**, 2569-2577 (2009).
16. Cleland, E. E., Chiariello, N. R., Loarie, S. R., Mooney, H. A. & Field, C. B. Diverse responses of phenology to global changes in a grassland ecosystem. *Proc. Natl. Acad. Sci. USA* **103**, 13740-13744 (2006).
17. Wang, H., Dai, J., Zheng, J. & Ge, Q. Temperature sensitivity of plant phenology in temperate and subtropical regions of China from 1850 to 2009. *Int. J. Climatol.* **35**, 913-922 (2015).
18. Chuine, I. M., Xavier; Bugmann, Harald. Warming, Photoperiods, and Tree Phenology. *Science* **329**, 277-278 (2010).
19. Chuine, I. A unified model for budburst of trees. *J. Theor. Biol.* **207**, 337-347 (2000).
20. Murray, M., Cannell, M. G. R. & Smith, R. I. Date of budburst of fifteen tree species in Britain following climatic warming. *J. Appl. Ecol.* **26**, 693-700 (1989).
21. Man, R., Lu, P. & Dang, Q. L. Insufficient Chilling Effects Vary among Boreal Tree Species and Chilling Duration. *Front Plant Sci* **8**, 1354, doi:10.3389/fpls.2017.01354 (2017).
22. Cannell, M. G. R. & Smith, R. I. L. Thermal time, chill days and prediction of budburst in Picea sitchensis. *J. Appl. Ecol.* **20**, 951-963 (1983).

23. Fu, Y. H. *et al.* Increased heat requirement for leaf flushing in temperate woody species over 1980-2012: effects of chilling, precipitation and insolation. *Glob. Change Biol.* **21**, 2687-2697 (2015).
24. Zhang, H., Liu, S., Regnier, P. & Yuan, W. New insights on plant phenological response to temperature revealed from long-term widespread observations in China. *Glob. Change Biol.* **24**, 2066-2078 (2018).
25. Yu, H., Luedeling, E. & Xu, J. Winter and spring warming result in delayed spring phenology on the Tibetan Plateau. *Proc. Natl. Acad. Sci. USA* **107**, 22151-22156 (2010).
26. Asse, D. *et al.* Warmer winters reduce the advance of tree spring phenology induced by warmer springs in the Alps. *Agric. For. Meteorol.* **252**, 220-230 (2018).
27. Ettinger, A. K. *et al.* Winter temperatures predominate in spring phenological responses to warming. *Nat. Clim. Change* **10**, 1137-1142. (2020).
28. Chuine, I. & Régnière, J. Process-Based Models of Phenology for Plants and Animals. *Annual Review of Ecology, Evol. Syst.* **48**, 159-182. (2017).
29. Caffarra, A., Donnelly, A., Chuine, I. & Jones, M. B. Modelling the timing of Betula pubescens budburst. I. Temperature and photoperiod: a conceptual model. *Clim. Res.* **46**, 147-157 (2011).
30. Luterbacher, J., Dietrich, D., Xoplaki, E., Grosjean, M. & Wanner, H. European Seasonal and Annual Temperature Variability, Trends, and Extremes Since 1500. *Science* **303**, 1499-1503 (2004).
31. Ciais, P. *et al.* in *Climate Change 2013: The Physical Science Basis. Contribution of Working Group I to the Fifth Assessment Report of the Intergovernmental Panel on Climate Change* (eds T.F. Stocker *et al.*) (Cambridge University Press, Cambridge, United Kingdom and New York, NY, USA, 2013).
32. Fu, Y. H. *et al.* Daylength helps temperate deciduous trees to leaf-out at the optimal time. *Glob. Change Biol.* **25**, 2410-2418 (2019).
33. Wolkovich, E. M. *et al*. A simple explanation for declining temperature sensitivity with warming. *Glob. Change Biol*. **27**, 4947-4949 (2021)
34 Templ, B. *et al.* Pan European Phenological database (PEP725): a single point of access for European data. *Int. J. Biometeorol.* **62**, 1109-1113 (2018).
35. Kramer, K. Selecting a model to predict the onset of growth of Fagus sylvatica. *J. Appl. Ecol.* **31**, 172-181 (1994).
36. Chuine, I., Cour, P. & Rousseau, D.-D. Selecting models to predict the timing of flowering of temperate trees: implications for tree phenology modelling. *Plant Cell and Environ.* **22**, 1-13 (1999).
37. Savas, R. Investigations on the annual cycle of development of forest trees. II. Autumn dormancy and winter dormancy. *Communicationes Instituti Forestalis. Fenniae* **84**, Helsinki (1974).
38. Hänninen, H. Modelling bud dormancy release in trees from cool and temperate regions. *Acta For. Fenn.* **14**, 499-454 (1990).
39. Harrington, C. A., Gould, P. J. & St. Clair, J. B. Modeling the effects of winter environment on dormancy release of Douglas-fir. *For. Ecol. Manag*. **259**, 798-808 (2010).
40. Zhang, H., Yuan, W., Liu, S., Dong, W. & Fu, Y. Sensitivity of flowering phenology to changing temperature in China. *J. Geophys. Res.: Biogeosci.* **120**, 1658-1665 (2015).
41. Richardson, A. D. *et al.* Influence of spring phenology on seasonal and annual carbon balance in two contrasting New England forests. *Tree Physiol.* **29**, 321-331 (2009).
42. Piao, S. *et al*. Plant phenology and global climate change: Current progresses and challenges. *Glob. Change Biol*. **25**, 1922-1940 (2019).
43. Körner, C. & Basler, D. Phenology Under Global Warming. *Science* **327**, 1461-1462 (2010).

44. Zohner, C. M. & Renner, S. S. Common garden comparison of the leaf-out phenology of woody species from different native climates, combined with herbarium records, forecasts long-term change. *Ecol. Lett.* **17**, 1016-1025 (2014).
45. Vitasse, Y. & Basler, D. What role for photoperiod in the bud burst phenology of European beech. *Eur. J. Fo. Res.* **132**, 1-8 (2012).
46. Lenz, A., Hoch, G., Körner, C. & Vitasse, Y. Convergence of leaf-out towards minimum risk of freezing damage in temperate trees. *Funct. Ecol.* **30**, 1480-1490 (2016).
47. Wang, Y. *et al*. Forest controls spring phenology of juvenile Smith fir along elevational gradients on the southeastern Tibetan Plateau. *Int. J. Biometeorol.***11**, 1031 (2019).
48. Marquis, B., Bergeron, Y., Simard, M. & Tremblay, F. Probability of sping frosts, not growing degree-days, drives onset of spruce bud burst in plantations at the boreal-temperate forest ecotone. *Front. Plant Sci.* **132**, 1-8 (2020); doi: 10.3389/fpls.2020.01031
49. Shen, M. Piao, S., Cong, N., Zhang, G. & Jassens, I.A. Precipitation impacts on vegetation spring phenology on the Tiberan Plateau. *Glob. Change Biol.* **21**, 3647-3656 (2015).
50. Liu, *et al*. Temperature, precipitation, and insolation effects on autumn vegetation phenology in temperate China. *Glob. Change Biol.* **22**, 644-655 (2016).
51. Minder, J. R., Mote, P. W. & Lundquist, J. D. Surface temperature lapse rates over complex terrain: Lessons from the Cascade Mountains. *J. Geophys. Res.* **115**, D14122 (2010); doi:10.1029/2009JD013493
52. Navarro-Serrano, *et al*. Elevation effects on air temperature in a topographically complex mountain valley in the Spanish Pyrenees. *Atmosphere*, **11**, 656 (2020); doi:10.3390/atmos11060656

Methods

Phenological and climatic data. Phenological datasets of LUD for the period 1951–2019, as well as the geographical location and elevation for each observation site, were obtained from the Pan European Phenology (PEP) network (http://www.pep725.eu), an open access repository of *in situ* phenological records for multiple plant species across Europe[34]. The LUDs were defined by the BBCH (Biologische Bundesanstalt, Bundessortenamt und Chemische Industrie) code as stage 11 (first leaf unfold). Specifically, we selected the LUD records of the six most observed tree species at 2,944 sites in central Europe (Table S1 and Extended Data Fig. 1). For each species, only the sites with phenological observations of at least 40 years were included in our analysis. The median absolute deviation (MAD) method[53,54] was then used to identify and exclude potentially erroneous records of LUD. For each species at each site, the MAD was calculated as: MAD = median ($|LUD_i$ – median (LUD_1, LUD_2, … $LUD_n)|$), where 1, 2, i and n are the 1st, 2nd, ith and nth observation years, respectively. Any record deviating by more than three times the MAD was considered as an outlier and removed from the original dataset used in this study. After MAD pre-treatment, 386,320 records of LUD remained for further analysis (Table S1). Distribution of these records across 1951–2019 is given in Extended Data Fig. 1b.

Daily mean air temperature at each site was obtained from the gridded database E-OBS (http://ensembles-eu.metoffice.com) at a spatial resolution of 0.1° (approx. 10 km)[55]. Due to the relatively coarse spatial resolution of the E-OBS database, the elevation of some phenological sites may be different greatly from the mean elevation of the grid cells (also obtained from the E-OBS database) where they locate, especially in mountainous areas. To reach a more accurate quantification of

547 temperature at each site, the temperature data from E-OBS were adjusted using the
548 difference between the actual elevation at each site (as specified in the PEP database)
549 and the mean elevation of the corresponding grid cell (as specified in E-OBS). The
550 temperature lapse rate is set to –0.64°C per 100 m increase in elevation[56].

551 **The Unified phenology model.** Phenological models are generally developed based
552 on distinct assumptions regarding the response of bud growth to spring thermal
553 accumulation and/or winter chilling[35,36]. For example, the Thermal Time model
554 considers that only forcing temperatures explain the leaf unfolding[22]. More
555 sophisticated models also consider the effect of chilling temperatures on bud
556 dormancy. For example, the Sequential model assumes that the effect of forcing
557 temperatures cannot be effective unless chilling requirements have already been
558 fulfilled[38]. In contrast, the Parallel model assumes that forcing temperatures can be
559 active concomitantly with chilling accumulation[35]. Furthermore, other models, such as
560 the Alternating model, assume that the thermal accumulation required for leaf
561 unfolding declines exponentially with increasing chilling accumulation[20]. These
562 models are non-nested (within each other) and, therefore, cannot be used to test the
563 effects of the above assumptions on the response of leaf unfolding to chilling and
564 forcing temperatures simultaneously[19]. To circumvent these limitations, we applied
565 the Unified phenology model[19] in our study.

566 The Unified model considers two phases of bud development, like the most complex
567 models that have been developed. These phases can overlap in time, as assumed in the
568 Parallel model; the second phase can also depend on the first phase, as assumed in the
569 Alternating model[20]. Most important, depending on the parameter estimates obtained
570 with the data, these assumptions can show support or not from the observation data
571 and the model can be simplified accordingly, for example in a Sequential model[38].

572 Similarly, the response functions to temperature during chilling and forcing stages can
573 be simplified in other functions which have been widely used as explained in Fig S6.
574 Overall, the model used integrates the main assumptions of simpler phenology
575 models, in particular the Sequential[38], Parallel[35] and Alternating[20] models, which can
576 be regarded as particular cases of the Unified model. For a complete explanation of
577 the relationship between the Unified model and earlier simpler models, see the
578 reference publication by Chuine (2000)[19].

579 The Unified phenology model[19] allows for a direct estimation of the response of
580 spring phenology to both chilling and forcing temperatures, and of the periods when
581 these temperatures affect the plant phenology. In the Unified model, the daily chilling
582 rate (CH_r, unitless) during cold days is calculated using a unimodal function (Fig.
583 S1a) of daily mean air temperature (T, °C):

584 $$CH_r = \frac{1}{e^{c_1(T-T_{op})^2 + c_2(T-T_{op})}} \quad (1)$$

585 where T_{op} is the optimal chilling temperature, and c_1 and c_2 are two calibration
586 coefficients (Table S2). With specific values of T_{op}, c_1 and c_2, Eq. (1) can capture
587 other widely used chilling metrics[19], such as, the chilling days (CH_r = 1 if T $\leqslant$ 5°C;
588 CH_r = 0 if T > 5°C) (Fig. S6a) and the chilling unit based on the triangular function
589 (Fig. S6b). Bud dormancy is released (d_{f0}) when the accumulation of daily chilling
590 rate since a specific day (d_{c0}, the start day of chilling accumulation) exceeds the
591 plants' critical chilling requirement (CHA_0, unitless), i.e. when $\sum_{d_{c0}}^{d_{f0}} CH_r > CHA_0$.
592 Note that d_{f0} also corresponds to the start day of forcing (thermal) accumulation (Fig.
593 S1). The daily forcing rate (F_r, unitless) is calculated using a sigmoid function (Fig.
594 S1a) of daily mean air temperature (T, °C):

595 $$F_r = \frac{1}{1.0+e^{c_3(T-T_{50})}} \quad (2)$$

596 where T_{50} is the mid-response temperature that induces 50% of optimal growth in
597 forcing rate and is the inflection point of the function; and c_3 is a calibration
598 coefficient. Leaf unfolding occurs when the forcing accumulation ($\sum_{d_{f0}}^{LUD} F_r$) exceeds a
599 certain thermal requirement (TA_0) which declines exponentially with the total chilling
600 accumulation (CHA_{tot}) during the whole pre-growing season (i.e. period from the start
601 day of chilling accumulation to the LUD) (Fig. S1b in SI):

602 $$TA_0 = c_4\, e^{c_5\, CHA_{tot}} \quad (3)$$

603 $$CHA_{tot} = \sum_{d_{c0}}^{LUD} CH_r \quad (4)$$

604 where c_4 and c_5 are calibration coefficients. Note that, in the Unified model, chilling
605 temperature continues to have an effect on CHA_{tot} after dormancy break and forcing
606 requirement decreases as CHA_{tot} increases.

607 **Parameter estimation and model application.** Nine parameters of the Unified
608 model, including the start day of chilling accumulation (d_{c0}), the critical chilling
609 requirement for releasing bud dormancy (CHA_0), the optimal chilling temperature
610 (T_{op}), the mid-response temperature (T_{50} in Eq. 2) and the five coefficients c_1 to c_5 in
611 Eqs. 1–3, were optimized for each species at each site using an effective global
612 optimization algorithm–the shuffled complex evolution algorithm (SEC-UA)[57]. Prior
613 values and the range of each parameter to be optimized are listed in Table S2. Root
614 mean square error (RMSE, Eq. 5) between simulated (LUD_{sim_i}) and observed
615 (LUD_{obs_i}) LUD was used as the objective function, and parameter values that
616 minimized the RMSE were regarded as optimal.

$$RMSE = \sqrt{\left(\frac{\sum_{i=1}^{n}(LUD_{sim\_i} - LUD_{obs\_i})^2}{n}\right)} \quad (5)$$

where n is the number of records (years) for each species at each site; and i is the rank of the observation year.

Using the optimized parameters, the Unified model was then applied to estimate the day of bud dormancy release, total chilling accumulation, daily forcing rate and the LUD for each year, species and site. We divided the whole 1951–2019 period into three shorter timespans: 1951–1979 (the reference period), 1980–1999 and 2000–2019. Analysis of the time series of LUD, mean winter temperature and mean spring temperature showed that the LUD and temperatures overall were stable in Europe during 1951–1979 (Figs. S9 & S10). In the 1980–1999 period, the spring temperature in Europe increased significantly and the LUD advanced quickly, by up to 0.5 day yr^{-1}. Then, in 2000–2019, the spring temperature in Europe was stable again overall, while winter temperature increased significantly (Figs. S9 & S10). For each of these three timespans, in addition to the average LUD and spring and winter temperatures, we calculated the metrics needed to represent winter chilling (i.e. CH_r and CHA_{tot}) and spring forcing (i.e. F_r and TA_0). The changes in each variable for each tree species at each site were then calculated, and the significance of changes was evaluated using the one-sample t-test (i.e. test whether the changes are significantly different from zero). The significance of difference between changes from 1951–1979 to both 1980–1999 and 2000–2019 was evaluated using the paired-sample t-test.

In the Unified model, the LUD is determined by the time when bud dormancy is released (which itself depends on the rate of chilling accumulation), the rate of forcing accumulation and the amount of forcing (TA_0) required for leaf unfolding (Fig. S1). To assess the relative contributions of these three factors to the temporal shifts in

LUD, we expressed their effects in number of days. We first calculated the changes in the date of bud dormancy break (d_{f0} in Fig. S1c) from the period 1951–1979 (d_{f0_1970s}) to periods 1980–1999 (d_{f0_1990s}) and 2000–2019 (d_{f0_2010s}) (Eqs. 6 & 7) for each tree species at each site (ΔD_{df0}, Figs. 2 & Extended Data 2):

$$\Delta D_{df0\_1990s} = d_{f0\_1990s} - d_{f0\_1970s} \quad (6)$$

$$\Delta D_{df0\_2010s} = d_{f0\_2010s} - d_{f0\_1970s} \quad (7)$$

Second, to estimate the shifts in LUD caused by the increased thermal accumulation (ΔD_{TA0} in Fig. 1) required for leaf unfolding due to warming-induced loss of winter chilling, we simulated the LUD for each species at each site for the two more recent timespans (1980–1999 and 2000–2019) by fixing the TA_0 in the Unified model to the average TA_0 corresponding to the reference period. From the reference period to the 1980–1999 and 2000–2019 periods, the ΔD_{TA0} was calculated as the difference between the simulated LUDs using the reference TA_0 (LUD_{TA0_1970s}) and those calculated based on the actual total winter chilling accumulation for each period using Eq. (3) (i.e. LUD_{TA0_1990s} and LUD_{TA0_2010s}) (Eqs. 8 & 9):

$$\Delta D_{TA0\_1990s} = LUD_{TA0\_1990s} - LUD_{TA0\_1970s} \quad (8)$$

$$\Delta D_{TA0\_2010s} = LUD_{TA0\_2010s} - LUD_{TA0\_1970s} \quad (9)$$

Third, the contribution of warming-induced changes in daily forcing rates to shifts in LUD (ΔD_{Fr}) was calculated as the change in the duration of the forcing stage (FD, i.e. the number of days from d_{f0} to LUD) from the reference period 1951–1979 (FD_{1970s}) to the periods 1980–1999 (FD_{1990s}) and 2000–2019 (FD_{2010s}), but excluding the influence of TA0 changes on this temporal shift (Eqs. 10 & 11):

$$\Delta D_{Fr\_1990s} = FD_{1990s} - FD_{1970s} - \Delta D_{TA0\_1990s} \quad (10)$$

$$\Delta D_{Fr\_2010s} = FD_{2010s} - FD_{1970s} - \Delta D_{TA0\_2010s} \quad (11)$$

Finally, the relative contributions of ΔD_{df0} ($p\Delta D_{df0}$), ΔD_{Fr} ($p\Delta D_{Fr}$) and ΔD_{TA0} ($p\Delta D_{TA0}$) to the shifts in LUD were calculated as follows:

$$p\Delta D_{df0} = \left(\frac{|\Delta D_{df0}|}{|\Delta D_{df0}|+|\Delta D_{FD}|+|\Delta D_{TA0}|}\right) \times 100 \quad (12)$$

$$p\Delta D_{FD} = \left(\frac{|\Delta D_{FD}|}{|\Delta D_{df0}|+|\Delta D_{FD}|+|\Delta D_{TA0}|}\right) \times 100 \quad (13)$$

$$p\Delta D_{TA0} = \left(\frac{|\Delta D_{TA0}|}{|\Delta D_{df0}|+|\Delta D_{FD}|+|\Delta D_{TA0}|}\right) \times 100 \quad (14)$$

Temperature sensitivity of LUD. The temperature sensitivity of LUD (S_T, day °C^{-1}) was first calculated for each species at each site based on a linear least square regression analysis of LUD and mean pre-season temperature, defined as the period from the start date of chilling accumulation (d_{c0} in Fig. 3) to the mean LUD. The slope of the linear regression line was then used to quantify S_T. In addition, we also calculated, from 1951 to 2019, the S_T when the pre-season for each species at each site is defined as the period (with 5-day steps) for which the absolute value of the correlation coefficient between LUD and air temperature was highest, i.e. the period which is most relevant to leaf unfolding[7]. In this case, we first calculated the mean temperature during each of the 27 periods ranging from 20 to 150 days (i.e. 20, 25, … , 145, 150, each at 5 day intervals) preceding the mean LUD. Pearson's correlation coefficient was calculated between the LUD and the mean temperature for each of these 27 periods. The period for which the absolute value of correlation coefficient between LUD and mean air temperature was highest was regarded as the optimal pre-season.

To estimate the trend in the temporal change of the temperature sensitivity of LUD, we also conducted a reduced major axis regression for each species at each site with a 15-year moving window from 1951 to 2019, that is, we calculated the temperature sensitivity for each continuous 15 years over the entire record period.

Photoperiod effect. To explore the potential uncertainties resulting from the neglecting the photoperiod in the Unified model, we compared the performance of the default Unified model (described above) against a revised version that represents the photoperiod effect. The comparison was performed using the model's ability to capture capture the observed LUD as a minimum criterion. In the revised model, the daily forcing rate (F_r) was calculated based on both daily mean air temperature (T, °C) and daily photoperiod (P, hours):

$$F_r = \frac{1}{1.0+e^{c_3(T-T_{50})}}\left(\frac{P}{10}\right)^e \quad (15)$$

where the temperature factor (Eq. 2) is identical to that in the default Unified model. The photoperiod factor ($\left(\frac{P}{10}\right)^e$) was obtained from Bluemel & Chmielewski (2012) [58] with e as a model parameter. The methodology for optimizing the free parameters in the revised Unified model was identical to that used in the default Unified model. The range for optimizing the parameter e was set to 0–5 with a prior value of 1.56. The revised Unified model was then applied to *Fagus sylvatica*, which has been reported to be one of the most sensitive species to photoperiod[44,45]. The performances of both the default and the revised Unified models in capturing LUDs was evaluated using the RMSE (Eq. 5) and the Akaike information criterion (AIC, Eq. 16), which considers both the goodness of fit and the number of free model parameters (n_{param}):

$$AIC = n \times ln\left(\frac{\sum_{i=1}^{n}(LUD_{sim\_i}-LUD_{obs\_i})^2}{n}\right) + 2n_{param} \quad (16)$$

where n is the number of records (years) for each species at each site; and LUD_{sim_i} and LUD_{obs_i} are the simulated and observed LUD in the year i, respectively.

Data availability

Phenology data are available from the Pan European Phenology (PEP) network (http://www.pep725.eu). Climate data can be downloaded from E-OBS site: http://ensembles-eu.metoffice.com.

Code availability

The codes of the Unified model and the program (SCE-UA algorithm) used for parameterization and data analysis can be found at https://github.com/hchzhang/UnifiedModel.git.

Method feferences

53. Chen, L. *et al.* Leaf senescence exhibits stronger climatic responses during warm than during cold autumns. *Nat. Clim. Change* **10**, 777-780 (2020).
54. Leys, C., Ley, C., Klein, O., Bernard, P. & Licata, L. Detecting outliers: Do not use standard deviation around the mean, use absolute deviation around the median. *J. Exp. Soc. Psychol.* **49**, 764-766 (2013).
55. Beer, C. *et al.* Harmonized European Long-Term Climate Data for Assessing the Effect of Changing Temporal Variability on Land–Atmosphere CO2 Fluxes. *J. Clim.* **27**, 4815-4834 (2014).
56. Olsson, C. & Jönsson, A. M. Process-based models not always better than empirical models for simulating budburst of Norway spruce and birch in Europe. *Glob. change biol.* **20 11**, 3492-3507 (2014).
57. Duan, Q., Sorooshian, S. & Gupta, V. K. Optimal use of the SCE-UA global optimization method for calibrating watershed models. *J. Hydrol.* **158**, 265-284 (1994).
58. Bluemel, K. & Chmielewski, F. Shortcomings of classical phenological forcing models and a way to overcome them. *Agric. For. Meteorol.*, **164**, 10-19 (2012).